



Stress in electroplated gold on silicon substrates and its dependence on cathode agitation[☆]



Suan Hui Pu^{*}, Andrew S. Holmes, Eric M. Yeatman

Department of Electrical and Electronic Engineering, Imperial College London, South Kensington Campus, London SW7 2AZ, UK

ARTICLE INFO

Article history:

Received 12 December 2012
Received in revised form 21 April 2013
Accepted 28 May 2013
Available online 5 June 2013

Keywords:

Gold electroplating
Cathode agitation
Residual stress

ABSTRACT

The influence of cathode agitation on the residual stress of electroplated gold has been investigated. Using a custom-built plating cell, a periodic, reciprocating motion was applied to silicon substrates that were electroplated with soft gold. A commercially available gold sulfite solution was used to deposit the 0.6 μm thick gold films using a current density of 3.0 mA/cm^2 and a bath temperature of 50 $^\circ\text{C}$. By increasing the speed of cathode agitation from 0 to 5 cm/s , the magnitude of the compressive stress decreased from -64 to -9 MPa. The results suggest that cathode agitation significantly alters the mass transport within the electrolytic cell and can be used as a method of stress control in gold electroplating. This finding is potentially significant for plating applications in microelectronics and microsystems that require precise stress control.

© 2013 The Authors. Published by Elsevier B.V. All rights reserved.

1. Introduction

Electroplated gold is a widely used material in the microelectronic and microsystems industries [1,2]. For many applications, the properties of gold such as its high electrical conductivity, low hardness and resistance to oxidation are often advantageous. For example, transmission lines in microwave integrated circuits are typically fabricated using gold to reduce signal attenuation [3]. In electronic assembly, soft gold is important for wire bonding and innovative flip-chip assembly [4,5]. Conversely, for applications such as electrical connectors or switch contacts, gold deposits with high hardness are important for achieving good wear resistance [2]. Relative to other deposition methods such as evaporation or sputtering, electroplating gives higher deposition rates and is particularly well suited to depositing thick films that are up to a hundred microns thick. In addition, a patterned photoresist mold is typically used in gold electroplating for microelectronic applications. This reduces material wastage since only the exposed device areas are deposited with gold whereas physical vapour deposition methods involve blanket deposition, followed by patterning using lift-off or etching using a photoresist mask. Another advantage of gold electroplating is that a wide range of gold electrolytes are available commercially, allowing the physical

properties of the gold deposit such as hardness, roughness and stress to be tailored.

For most gold plating processes, the deposits contain residual stresses that can be either compressive or tensile, depending on the plating parameters. Stress control in gold plating is particularly critical in applications such as mask fabrication in X-ray lithography [6–10]. X-ray lithographic masks consist of gold absorber patterns deposited on thin membranes only a few microns thick [6,9]. As the gold layer can be up to one micron thick, residual stresses can result in significant bending moments, causing mask distortion and poor pattern transfer. For radio frequency MEMS (micro-electromechanical systems) applications, fixed–fixed beam structures are often employed as switches [11]. An increase in the switching voltages can occur when a severe state of residual tension is built into the beams. This causes a stiffening effect and results in a deviation from designed switching voltages. Residual stress control in gold films can also be used to fabricate curved, electrostatically-actuated electrodes [12,13]. For example, a curved cantilever electrode can be achieved using a bilayered gold–copper structure [13]. The gold bottom layer is electroplated using a relatively stress-free process while the top copper layer is deposited with residual tension.

In previous work, the stress of electroplated gold has been reported as a function of plating current density [6–8,10,14], bath temperature [8,10], film thickness [6,8], pulsed-current plating [6,9,14], and the addition of brighteners such as arsenic [14] or thallium [10]. In this work, the influence of direct cathode (substrate) agitation on stress in soft, pure gold is studied experimentally. In all forms of electroplating, mass transport plays a key role in the properties of the electroplated film [15]. To obtain electrolyte mixing and ion replenishment in the vicinity of the

[☆] This is an open-access article distributed under the terms of the Creative Commons Attribution License, which permits unrestricted use, distribution, and reproduction in any medium, provided the original author and source are credited.

^{*} Corresponding author. Present address: University of Southampton (USMC), No. 3, Persiaran Canselor 1, Kota Ilmu Educity @ Iskandar, 79200 Nusajaya, Johor, Malaysia. Tel.: +60 7 560 2 461.

E-mail address: suanhui.pu@soton.ac.uk (S.H. Pu).

wafer, commercial plating baths employ continuously pumped electrolytic cells that are filtered using submicron filters. In laboratory plating equipment, electrolyte agitation is often induced using magnetic stirrers in small scale plating cells. The use of periodic, reciprocating cathode agitation as a means of enhancing mass transport in gold electroplating has not been explored systematically. Our results suggest that the residual stress in electroplated gold can be controlled by adjusting the speed of cathode agitation.

2. Experimental details

A commercially available gold sulfite solution (Metalor ECF 60) was used for the electroplating experiments. For microelectronic applications, sulfite-based gold plating solutions offer better compatibility with positive photoresists relative to cyanide-based solutions [14,16,17]. Gold cyanide solutions tend to attack positive photoresists, causing underplating at the interface between the resist and the seed layer. Due to the limitations in pattern transfer quality, cyanide-based solutions are seldom employed in microelectronics fabrication. In the experiments, the pH of the gold sulfite solution was maintained at 9.5 and no brightener or grain refiner was added to the solution. Soft gold was deposited on silicon substrates that were pre-coated with a gold seed layer. The stress of the electroplated gold was then measured for a range of cathode agitation speeds, plating temperatures and current densities.

2.1. Cathode agitation

Previously, the effect of cathode vibration (in a direction parallel to the anode) on mass transport has been studied in copper electrolytic cells [18,19]. For vibration amplitudes up to 8 mm and frequencies up to around 50 Hz, the results showed a significant increase in the mass transfer coefficient. In order to enhance mass transport in gold electroplating, a custom-built electroplating cell that allows periodic cathode agitation was used in the current work [20]. As shown in Fig. 1, the samples were mounted on a polypropylene sample holder that was attached to a reciprocating slider–crank mechanism. A platinized titanium anode was mounted parallel to the cathode and a separation of 40 mm was maintained between the electrodes.

Cathode agitation was achieved using a DC motor to actuate the slider–crank mechanism. The instantaneous linear velocity of the sample is sinusoidal and given by

$$v \approx r\omega \sin(\omega t) \quad (1)$$

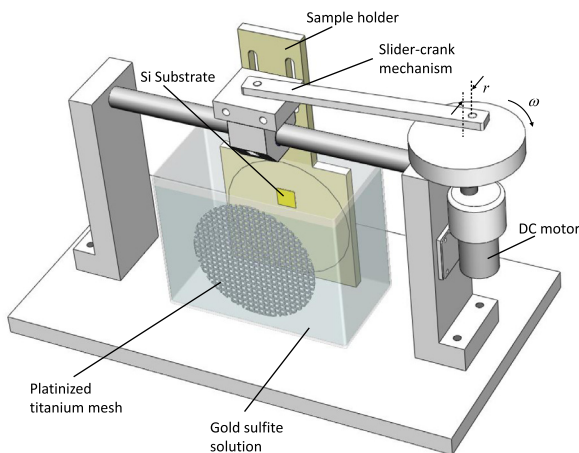


Fig. 1. Electroplating cell with reciprocating cathode agitation.

where r and ω are the radius and angular velocity of the crank, respectively. The corresponding root mean square speed of the sample is

$$v_{\text{rms}} \approx \frac{r\omega}{\sqrt{2}} \quad (2)$$

2.2. Stress measurement

The stress in the electroplated gold was measured using silicon cantilevers fabricated on 4-inch silicon-on-insulator (SOI) wafers. For the experiments, the silicon wafers were diced into smaller chips with 16 cantilevers per chip. Each cantilever is 3000 μm long, 200 μm wide and 20 μm deep. The edges of the cantilevers are aligned with the Si $\langle 100 \rangle$ lattice directions. A thin, 150 nm gold seed layer is sputtered onto the top surface of the cantilever prior to gold electroplating. Fig. 2 shows a typical chip with the silicon cantilevers for stress measurement.

The height of each cantilever tip was measured relative to the chip surface before and after gold electroplating. Cantilever height measurements were made using a Veeco Wyko NT9100 white light interferometer. A typical Wyko scan is shown in Fig. 3, where the positions A and B indicate the cantilever tip and the rigid chip surface, respectively. The difference in the initial and final cantilever heights gives the vertical displacement, δ due to the stress in the gold film.

For a given film stress, the curvature induced in the cantilever beam can be expressed using Stoney's equation [21], since the thickness of the gold deposit is much smaller than the thickness of the cantilever. Hence, the curvature is given by

$$\kappa \approx \frac{6h_f\sigma_f(1-\nu_s)}{E_s h_s^2} \quad (3)$$

where h_f and σ_f are the thickness and stress of the plated gold, respectively. E_s , h_s and ν_s are the Young's modulus, thickness and Poisson's ratio of the cantilever, respectively. The factor $(1-\nu_s)$ in Eq. (3), which is not present in Stoney's original formula, is due to the fact that the stress in the gold film is biaxial in nature [22]. Stoney's original formula assumed that the film stress is uniaxial. For displacements that are small relative to the cantilever length L ,

$$\frac{\partial^2 \delta}{\partial x^2} \approx \kappa \quad (4)$$

and the boundary conditions for the built-in end are

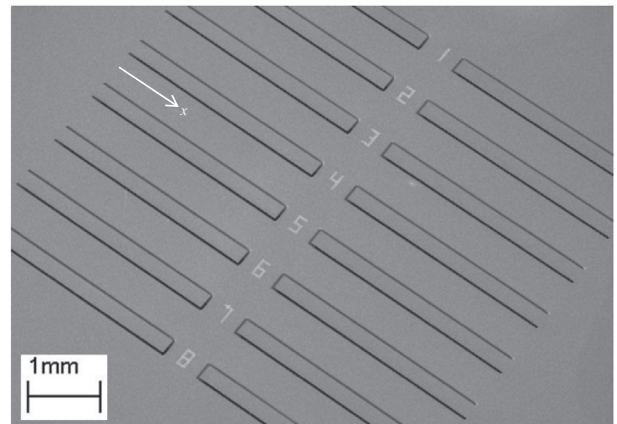


Fig. 2. Silicon cantilevers fabricated using an SOI process.

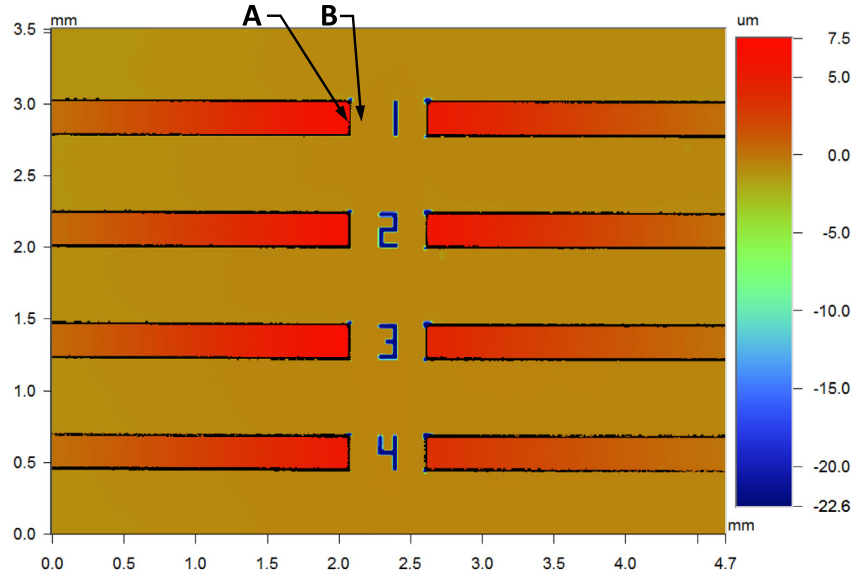


Fig. 3. A Wyko white light interferometer scan of a typical silicon cantilever chip.

$$\delta(0) = 0 \quad (5)$$

$$\left. \frac{\partial \delta}{\partial x} \right|_{x=0} = 0$$

By integrating Eq. (4), the vertical deflection of the beam can thus be expressed as

$$\delta(x) \approx \frac{1}{2} \kappa x^2 \quad (6)$$

The film stress is then obtained by combining Eq. (3) and Eq. (6) (for $x = L$), i.e.

$$\sigma_f \approx \frac{E_s h_s^2 \delta}{3 h_f L^2 (1 - \nu_s)} \quad (7)$$

In the experiments, the cantilever thickness h_s consists of the sum of the 20 μm thick silicon cantilever and the 150 nm thick gold seed layer. The Young's modulus of the cantilever E_s is taken to be 130 GPa, i.e. the value for Si <100> and the effect of the thin gold seed layer is assumed to be negligible. Similarly, the Poisson's ratio of the cantilever ν_s is taken to be 0.28. The thickness of the electroplated gold films h_f were measured by covering a small portion of each chip with photoresist and then stripping the exposed gold with a potassium ferricyanide etchant. The total gold thickness was measured with a stylus profilometer and h_f is the measured thickness less the thickness of the gold seed layer (150 nm).

3. Results

3.1. Current density

As a prelude to studying the stress of the electroplated gold as a function of cathode agitation, the influence of plating current density and solution temperature on film stress was explored. In these experiments, no mechanical agitation was employed to perturb the solution. Fig. 4 shows the influence of plating current on the film stress between the current density values of 1.0 and 5.0 mA/cm^2 . The bath temperature was maintained at 55 $^\circ\text{C}$ and the average film thickness was 0.7 μm . It was observed that the stress values were compressive with a range between -35 and -103 MPa. From the experimental data, a local maximum in compressive stress was obtained at around 3.0 mA/cm^2 .

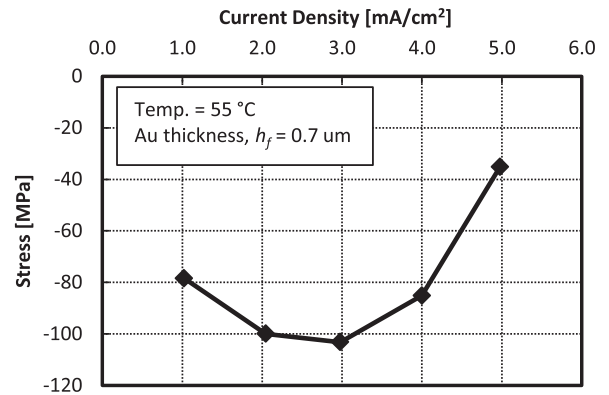


Fig. 4. Stress of soft gold on silicon versus current density.

The evolution of intrinsic stress in thin films is known to be dependent on several factors, including growth mechanism [23,24], evolution of grain morphology during deposition [8,14,23], and the inclusion of impurities [25,26]. In terms of growth mechanism, a mode that favours island nucleation followed by coalescence (to minimise surface energy) generates tensile stress. Conversely, a growth mode consisting of adatom incorporation into the grain boundaries generates compressive stress. It has been shown previously that film thickness affects the resulting stress in gold films [6,27] and this is likely due to the interplay of growth processes as well as grain development. For processes where impurities become incorporated into the gold film, this typically results in a volume expansion which then creates compressive stress. For example, it has been reported that gold films deposited using sulfite solutions can have significant porosity due to hydrogen co-deposition [14]. In practice, it is difficult to experimentally quantify the relative contributions of the above factors in the final film stress. In previously reported results, a wide range of stress values have been obtained in gold deposited using sulfite baths with values ranging from -100 to 100 MPa [6,7,9,10,14,16,28]. For the results in the current work, the compressive nature of the stress suggests that the variation in stress

with current density is most likely due to the effect of deposition rate on the resultant film morphology as well as hydrogen incorporation.

3.2. Bath temperature

Fig. 5 shows the dependence of film stress on the bath temperature. The current density was fixed at 3.0 mA/cm^2 and average film thickness was $0.6 \text{ }\mu\text{m}$. It was observed that the residual stress increased monotonically from -10 to -77 MPa when the plating temperature was increased from 22 to $60 \text{ }^\circ\text{C}$. In a previous study for gold plated onto silicon using a sulfite bath [10], stress values of -25 to 65 MPa were reported when the plating temperature was increased from 20 to $60 \text{ }^\circ\text{C}$. The main difference in the plating condition of the previous study was the inclusion of thallium (75 ppm) as a brightener. This is likely to be the root cause of the difference in stress formation with values ranging from mildly compressive to significantly tensile.

3.3. Cathode agitation

To measure the dependence of film stress on cathode agitation, the bath temperature was maintained at $50 \text{ }^\circ\text{C}$ and the films were deposited using a current density of 3.0 mA/cm^2 . The plating temperature and current values were the supplier's recommended plating conditions. The cathode agitation speed, v_{rms} ranged from 0 to 8.3 cm/s , and the peak to peak amplitude of the agitation was 30 mm ($r = 15 \text{ mm}$). In this experiment, the films were plated to a thickness of $0.6 \text{ }\mu\text{m}$.

Fig. 6 shows the stress magnitudes in the gold films with respect to the cathode agitation speed. With zero agitation, a film stress of -64 MPa was obtained. When v_{rms} was increased to 1.7 cm/s , the film stress decreased significantly to -20 MPa . Further decrease in the magnitude of the compressive stress was obtained by increasing v_{rms} from 1.7 to 5.0 cm/s . For v_{rms} between 5.0 and 8.3 cm/s , the stress value stabilizes at around -9 MPa .

3.4. Discussion

From the experimental results, introducing cathode agitation significantly reduced the stress of gold films deposited on silicon substrates using a gold sulfite solution. This suggests that cathode agitation can be used as a means of stress control in gold electroplating. Furthermore, for a plating temperature of $50 \text{ }^\circ\text{C}$ and a cathode agitation speed of 5.0 cm/s a very low stress value of -9 MPa was obtained. From the trend of stress magnitude versus agitation, the change in stress appears to plateau at 5.0 cm/s . Further

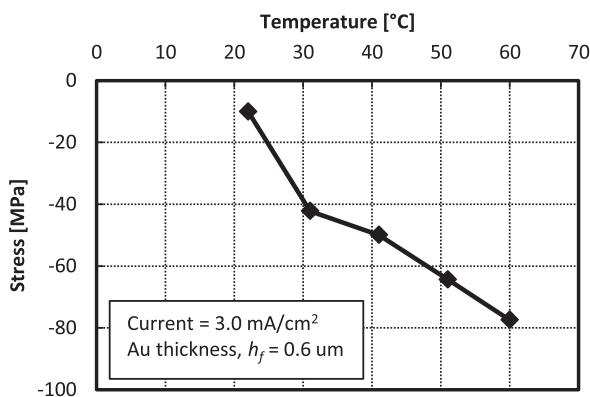


Fig. 5. Stress of soft gold on silicon versus bath temperature.

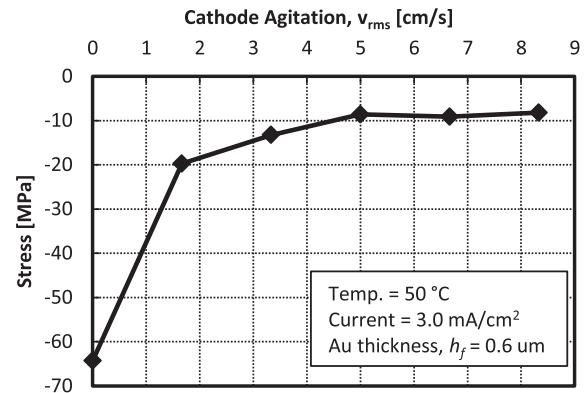


Fig. 6. Stress of soft gold on silicon versus cathode agitation speed.

increase in agitation speed did not produce any significant decrease in stress magnitude.

In this work, the direction of cathode agitation was chosen to be parallel rather than perpendicular to the face of the sample in order to obtain uniform electrolyte mixing at the cathode–electrolyte interface. In contrast, with perpendicular agitation, the edges of the sample are exposed to greater electrolyte mixing and hence increased mass transport relative to the centre. Parallel agitation is also expected to increase mass transport relative to a laminar flow plating cell due to the direct shearing of the cathode–electrolyte interface. In order to understand the effect of agitation on the electrolyte, the problem can be studied using the analytical solution for an infinite plate undergoing in-plane sinusoidal oscillation while immersed in a viscous fluid. This problem is generally known as Stoke's second problem, and the fluid velocity profile is given by [29].

$$u = Ue^{-ky} \sin(\omega t - ky) \quad (8)$$

where $U = r\omega$ is the peak velocity magnitude (from Eq. (1)), $k = \sqrt{(\omega/2\nu)}$ and ν is the kinematic viscosity of the fluid. The solution represents a strongly damped wave in the direction perpendicular to the plate. Fig. 7 shows the solutions for various cathode agitation speeds at the instant when $\omega t = \pi$. The kinematic viscosity value is estimated using the value for water at $50 \text{ }^\circ\text{C}$, i.e. $\nu = 0.55 \times 10^{-6} \text{ m}^2/\text{s}$. It can be observed that due to the damping factor, the effect of the oscillation on the fluid velocity is relatively confined to the plate surface (the separation between the anode and cathode is 40 mm). This could explain in part why the effect of the agitation on the film stress plateaus for $v_{\text{rms}} = 5.0 \text{ cm/s}$. For further insight into the effect of agitation on the mass transport to the cathode, a more detailed analysis is required. The analysis would need to take into account (i) the diffusion due to changes in the concentration of ions and (ii) the effect of the electric field on mass transport. Moreover, deviation from the ideal case of an infinite plate will also need to be accounted for, especially at the sample edges.

In many gold electroplating applications, the optimum plating temperature is between 40 and $60 \text{ }^\circ\text{C}$ in order to obtain the required film properties (e.g. brightness or density). Above-ambient plating temperatures can result in significant stresses induced by the mismatch between the thermal expansion coefficients of gold and the substrate. Hence, cathode agitation could play an important role in stress control for plating at high temperatures. It is important to note that the stress values reported in this paper are applicable to gold deposited on silicon substrates. Therefore, the stress values reported in this paper should only be directly compared to other results for gold deposited on silicon, for a given set of plating parameters.

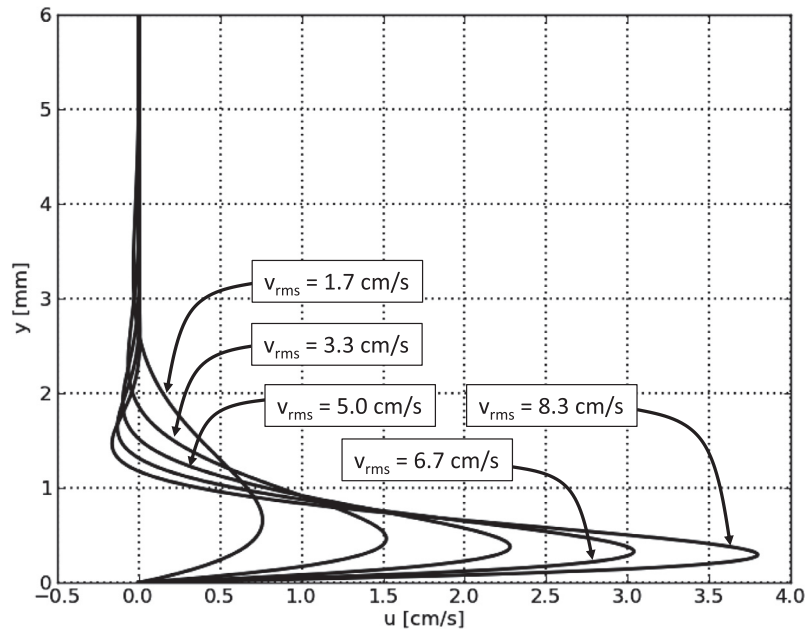


Fig. 7. Velocity profile at various agitation speeds (for $\omega t = \pi$).

The compressive nature of the stress obtained for all the experiments are consistent with previous work [16] where the ECF 60 gold sulfite solution was used to deposit gold films on silicon wafers. In the previous study, an intrinsic stress magnitude of the order of -20 MPa (excluding thermal component) was obtained using a flow cell plating configuration with a plating temperature of 45 °C and a plating current density of 3.5 mA/cm². The linear coefficients of thermal expansion for gold and silicon are 1.4×10^{-5} and 2.8×10^{-6} , respectively. This generates a tensile thermal stress component (after cooling) of 1 MPa/°C when plating at above-ambient temperature. In terms of roughness in the gold deposits, no correlation was observed with either current density, temperature or cathode agitation. For the film thickness range of 0.55 to 0.74 μ m, the roughness average values were of the order of 15 nm or less, indicating a very smooth surface.

For microelectronic or MEMS applications, the uniformity in deposit thickness across a wafer is important in order to have a robust process that meets device performance specifications. For plating configurations where non-uniform agitation is applied, it is possible to have large non-uniformities in the deposit thickness [7]. In preliminary results, 130 μ m by 130 μ m by 3.5 μ m gold bumps were electroplated using a photoresist mold on 4-inch glass wafers. Using an agitation speed of 3.3 cm/s, a plating current of 3.0 mA/cm² and a bath temperature of 50 °C, the bump heights were within 6% of the mean height. Furthermore, only a single electrical contact was used at the edge of the 4-inch wafer, and the uniformity results are comparable to previous work using gold sulfite plating solutions [16,30]. The results also show that gold deposits with high uniformity can be achieved and no adverse effect is observed due to cathode agitation.

4. Conclusions

The formation of stress in electroplated gold on a silicon substrate has been studied with respect to reciprocating cathode agitation. The results show that cathode agitation significantly reduced the magnitude of the compressive stress in the deposited films, relative to plating without cathode agitation. Cathode agitation can be used as a means of stress control in gold electroplating,

apart from adjusting the current density and bath temperature. Further work is required to study the mass transport of the gold within the electrolytic bath, in response to the cathode agitation. In addition, it would be interesting to study the influence of agitation on the microstructural properties of the gold films.

Acknowledgments

This work was funded by the UK Engineering and Physical Sciences Research Council (EPSRC) under the Flagship Project EP/D064805/1. The authors thank Mike Wild from Metalor Technologies (UK) for helpful discussions. We also gratefully acknowledge the assistance of Sunil Rana and Man Niang Kham with the optical interferometer measurements.

References

- [1] M. Kato, Y. Okinaka, *Gold Bull.* 37 (2004) 37–44.
- [2] T.A. Green, *Gold Bull.* 40 (2007) 105–114.
- [3] C.P. Wen, *IEEE Trans. Microwave Theory Tech.* 17 (1969) 1087–1090.
- [4] R. Holliday, P. Goodman, *IEE Rev.* 48 (2002) 15–19.
- [5] L.E.S. Rohwer, D. Chu, *IEEE Electron. Compon. Technol. Conf.* (2011) 907–910.
- [6] S.-L. Chiu, R.E. Acosta, *J. Vac. Sci. Technol. B* 8 (1990) 1589–1594.
- [7] W. Chu, M.L. Schattenburg, H.I. Smith, *Microelectron. Eng.* 17 (1992) 223–226.
- [8] B. Kebabi, C. Khan Malek, *J. Vac. Sci. Technol. B* 9 (1991) 154–161.
- [9] T. Ogawa, T. Soga, Y. Maruyama, H. Oizumi, K. Mochiji, *J. Vac. Sci. Technol. B* 10 (1992) 1193–1196.
- [10] W.J. Dauksher, D.J. Resnick, W.A. Johnson, A.W. Yanof, *Microelectron. Eng.* 23 (1994) 235–238.
- [11] C. Goldsmith, T.-H. Lin, B. Powers, W.-R. Wu, B. Norvell, *Micromechanical membrane switches for microwave applications*, in: *IEEE MTT-S Int. Microwave Symp. Dig.*, Orlando, FL, USA (1995) 91–94.
- [12] A.K. Chinthakindi, D. Bhusari, B.P. Dusch, J. Musolf, B.A. Willemsen, E. Prophet, M. Roberson, P.A. Kohl, *J. Electrochem. Soc.* 149 (2002) H139–H145.
- [13] S.H. Pu, A.S. Holmes, E.M. Yeatman, C. Papavassiliou, S. Lucyszyn, *J. Micromech. Microeng.* 20 (2010) 035030.
- [14] J.J. Kelly, N. Yang, T. Headley, J. Hachman, *J. Electrochem. Soc.* 150 (2003) C445–C450.
- [15] M. Datta, D. Landolt, *Electrochim. Acta* 45 (2000) 2535–2558.
- [16] T.A. Green, M.-J. Liew, S. Roy, *J. Electrochem. Soc.* 150 (2003) C104–C110.
- [17] A. Gemmler, W. Keller, H. Richter, K. Ruess, *High performance gold plating for microdevices*, in: *Proc. AESF SUR/FIN Annu. Int. Tech. Conf.*, Atlanta, GA, USA (1992) 553–573.
- [18] M.I. Ismail, A.M. Al-Taweel, M.Z. El-Abd, *J. Appl. Electrochem.* 4 (1974) 347–350.
- [19] M.-B. Liu, E.M. Rudnick, G.M. Cook, N.P. Yao, *J. Electrochem. Soc.* 129 (1982) 1955–1959.

- [20] S.H. Pu, A micromachined zipping variable capacitor, Imperial College London PhD Thesis, London, UK, 2010.
- [21] G.G. Stoney, Proc. R. Soc. London Ser. A 82 (1909) 172–175.
- [22] L.B. Freund, S. Suresh, Thin film materials; stress, Defect Formation and Surface Evolution, Cambridge University Press, Cambridge, U.K., 2004.
- [23] J.A. Floro, E. Chason, R.C. Cammarata, D.J. Srolovitz, MRS Bull. 27 (2002) 19–25.
- [24] R. Weil, Annu. Rev. Mater. Sci. 19 (1989) 165–182.
- [25] H. Angerer, N. Ibl, J. Appl. Electrochem. 9 (1979) 219–232.
- [26] D.L. Rehrig, N.V. Mandich, Trans. Inst. Met. Finish. 79 (2001) 160–162.
- [27] S. Kal, A. Bagolini, B. Margesin, M. Zen, Microelectron. J. 37 (2006) 1329–1334.
- [28] R.J. Morrissey, Plat. Surf. Finish. 80 (1993) 75–79.
- [29] J.A. Schetz, A.E. Fuhs, Fundamentals of Fluid Mechanics, Wiley, New York, 1999.
- [30] J. Simon, W. Zilske, F. Simon, The development of a high speed gold sulfite electrolyte for bumping, in: Proc. ITAP – Int. Symp. Flip Chip, Ball Grid Array, TAB and Adv. Packag., San Jose, CA, USA, 1995, pp. 275–289.